inorganics

MDPI

Perspective

Toward High-Performances of Halide Light-Emitting Diodes: The Importance of Ligands Engineering

Le Ma and Feijiu Wang *

Henan Key Laboratory of Photovoltaic Materials, Henan University, 1 Jinming Road, Kaifeng 475004, China; reckmale1220@163.com

* Correspondence: wangfeijiu@hotmail.com

Abstract: Halide perovskite light-emitting diodes (PeLEDs) have attracted great attention because of their superior optical properties, such as extremely high photoluminescence (quantum yield up to nearly 100%) of active layers with tunable wavelengths over the entire visible spectral range. With a suitable modification of halide perovskites, carrier transport materials, and their interfaces, external quantum efficiencies exceeding 10%, 25%, and 20% have been achieved for blue-colored (465 nm), green-colored (512 nm), and red-colored (640 nm) LEDs, respectively. Many strategies for pursuing high performances of devices have been successfully demonstrated, among which ligand engineering has always played an important role in the active layer. Herein, we present a perspective to illustrate the effects and roles of the ligands in cesium lead bromide light-emitting diodes. This perspective is mainly classified into three parts: (1) ligands for $CsPbBr_3$ LEDs could improve radiative recombination of perovskites and contribute to better efficiency of LEDs; (2) ligands could confine $CsPbBr_3$ growth for blue emission of LEDs; (3) stabilities of materials and devices become better with ligand engineering. Finally, the summary and perspective on PeLEDs are highlighted and possible solutions are provided.

Keywords: halide perovskite; light-emitting diodes; ligand engineering; $CsPbBr_3$ LEDs; stability

Citation: Ma, L.; Wang, F. Toward High-Performances of Halide Light-Emitting Diodes: The Importance of Ligands Engineering. *Inorganics* **2023**, *11*, 230. https://doi.org/10.3390/inorganics11060230

Academic Editor: Chiara Dionigi

Received: 12 April 2023
Revised: 4 May 2023
Accepted: 8 May 2023
Published: 26 May 2023

1. Introduction

Organic-inorganic hybrid perovskite (OIHP) LEDs have shown high performance because of their high photoluminescence quantum yield (PLQYs), high carrier mobility, and unique defect-tolerant nature [1–9]. However, phase instability of OIHP under moisture, heat, and even oxygen greatly limits their practical application because of the volatility of the organic components in perovskites (such as methylammonium (MA), formamidinium (FA), or mixed components) and the weak chemical bonding energies between halide anions (Cl^-, Br^-, or I^-) and metal cations (Pb^{2+}) [10–13]. Despite many strategies for improving stability, such as surface modification with stable materials [14,15], advanced encapsulation techniques [16–19], and compositional engineering [20–22], the intrinsic instability of hybrid perovskite materials is still a pending issue. $CsPbX_3$ (X = Cl^-, Br^-, or I^-), a type of all-inorganic perovskite, presents better stability than OIHP and possesses effective luminescence emission [17,23]. $CsPbBr_3$ has been extensively investigated in light-emitting-diode field because it could possess both green and blue emission by controlling the quantum confinement [24–28].

$CsPbBr_3$ with a chemical formula of ABX_3 has an octahedron structure, in which Pb and Br atoms form a corner-sharing $[PbBr_6]^{4-}$ 3-dimensional (3D) framework and Cs atoms occupy the octahedral voids (Figure 1a) [29,30]. The structural stability and distortion of $CsPbBr_3$ could be predicated by the Goldschmidt tolerance factor (τ), which is defined as $\tau = (R_{Cs} + R_{Pb})/\sqrt{2}(R_{Cs} + R_{Br})$, where R is the ionic radius. Generally, the cubic phase structure with the τ between 0.9 to 1 is considered the most stable structure, and $CsPbBr_3$ shows 0.92 of the value [31,32]. Additionally, $CsPbBr_3$ has three different

structural phases, which are called the cubic (α-, Pm-3m), tetragonal (β-, P4/mbm), and orthorhombic (γ-, Pnma) phase, respectively [33,34]. It is an γ-phase at room temperature, and its phase transitions happen when the temperature increases to 88 (β-phase) and 130 °C (α-phase) [35,36]. Luckily, the three phases of $CsPbBr_3$ have similar properties, which support a wide temperature operation range for the perovskite. $CsPbBr_3$ has been fundamentally investigated for its physics properties, such as absorption coefficient, carrier diffusion length, and carrier mobility [37–39]. For detailed information, many theoretical studies on the $CsPbBr_3$ were conducted, from which the band gap, absorption coefficient, carrier effective masses, and exciton binding energy could be extracted using the density functional theory (DFT) methods. A single crystal of the $CsPbBr_3$ exhibiting an absorbance coefficient of 10^5 cm^{-1}, a carrier diffusion length of 10 μm, and a carrier mobility of >100 cm^2 V^{-1} S^{-1} was reported [40,41], indicating its superiorities and potential for the optoelectronic devices such as LEDs. Note that electron and hole mobility in $CsPbBr_3$ are similar, implying that better carrier transport balance could be realized in the applications. Additionally, solution-processable techniques for the nanocrystal, nanoplatelet, quasi-two-dimensional (quasi-2D) layer, and 3D polycrystal of perovskite film formation have been applied in high brightness and EQE LEDs. With extensive and great developments, green $CsPbBr_3$ LEDs present very high performance with external quantum efficiencies (EQEs) exceeding 20% and outstanding brightness, which are comparable to organic and CdSe-based LEDs (Figure 1b) [42–46]. Rapid increases in LED performance have always involved strategies for defect passivation and carrier confinement in the active layer and improving injection/transport in devices [47–49]. The ligands, such as didodecyldimethylammonium bromide (DDAB), tetraoctylammonium bromide (TOAB), and n-butylammonium bromide (BABr), play vital roles to realize the above-mentioned strategies in the LEDs by controlling the on-substrate nanocrystal fabrication, forming quasi-2D perovskite, and modifying the perovskite surface [50–52].

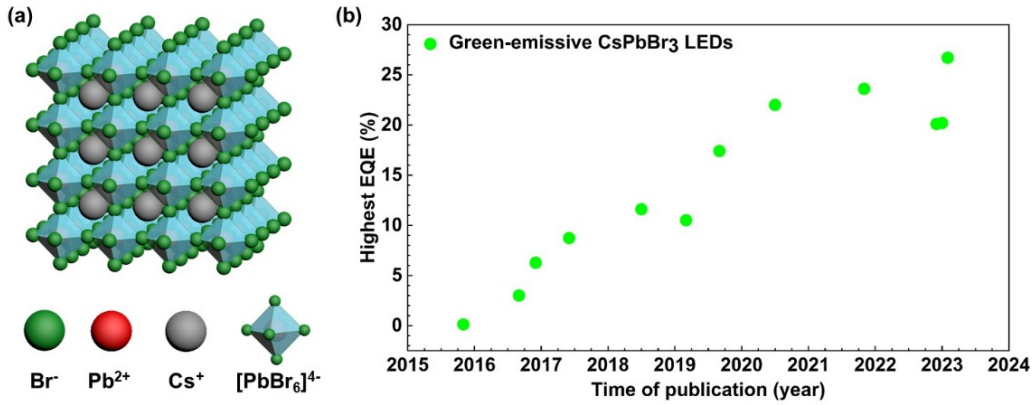

Figure 1. (**a**) Cubic structure of $CsPbBr_3$ perovskite; (**b**) evolution of external quantum efficiencies (EQEs) of green-LEDs employing $CsPbBr_3$-emitting layer. The EQE data was collected from references [43–45,47,48,50,52–57].

Here, we discuss strategies for achieving high performance of $CsPbBr_3$ LEDs through the ligand engineer's effective modification of stability, radiative recombination, and morphology of perovskites. We also overview challenges and possible solutions to realize highly efficient green and blue PeLEDs, including the external quantum efficiency and operational stability of devices.

2. Toward High Radiative Recombination of $CsPbBr_3$

Although the theoretical simulations demonstrated great defect tolerance of MHPs [58,59], the detrimental effect of defects on the perovskite LEDs was extensively reported. Several types of point defects containing vacancies, metallic Pb^0, and antisite substitutions were evidenced to be associated with nonradiative trap states (Figure 2a) [60,61].

Therefore, the reduction of trap states in perovskite to minimize trap-assisted nonradiative recombination is of great importance for improving the luminescence of the emitting layer. Ligands, including Lewis bases, ammonium, and halide salts, have been considered one of the most effective strategies for defect elimination because of their extra coordination or ionic bonding to the annihilation of trap states (Figure 2b) [62]. Lewis bases, such as amine and phosphine oxide, present significant passivation effects on perovskites because of their high binding affinity [45,62,63]. In addition, hydroxyl [64,65] and carboxyl [56] were reported to effectively control the $CsPbBr_3$ crystal size, surface coverage, and defect density, resulting in improved performance and stability of LEDs. Moreover, amine-based agents, such as 4-(2-aminoethyl)benzoic acid (ABA), DDAB, diamine-based molecules (Figure 2c), and even PMMA could effectively remove the metallic Pb site because of halide vacancy passivation-assisted suppression of metallic Pb, stripping of lead atoms, and weak hydrogen bonding with organic cations [62,66,67]. Besides the defect-induced nonradiative recombination, Auger recombination is also a nonradiative process, which is dominant at high excitation density [62]. This is one of the critical reasons for the efficiency roll-off with bias voltage increase in LEDs, especially in devices based on quantum-confined perovskite emitting layer because of the Auger recombination occurring at relatively low charge-carrier density (~10^{15} cm^{-3}, Figure 2d) [68]. For bulk perovskites, the Auger recombination–dominated process usually occurs at high excitation densities of >10^{17} cm^{-3} (Figure 2e), which indicates that high-power optoelectronic devices could probably be realized by bulk perovskites. Although quantum-confined perovskites could easily result in Auger recombination, the perovskite nanocrystals (PNCs) present very similar Auger recombination rates with bulk [39], indicating that PNCs are highly possible for high brightness and EQE LEDs. A further understanding of the Auger recombination mechanism is still needed in PNCs. It is worth noting that the ligands for passivation of the trap states, improvement of the crystallization, and even control of crystal growth usually employ short chain length with high binding affinity to perovskites, which not only easily passivates the trap state but also greatly reduces negative effects on the electrical properties for devices.

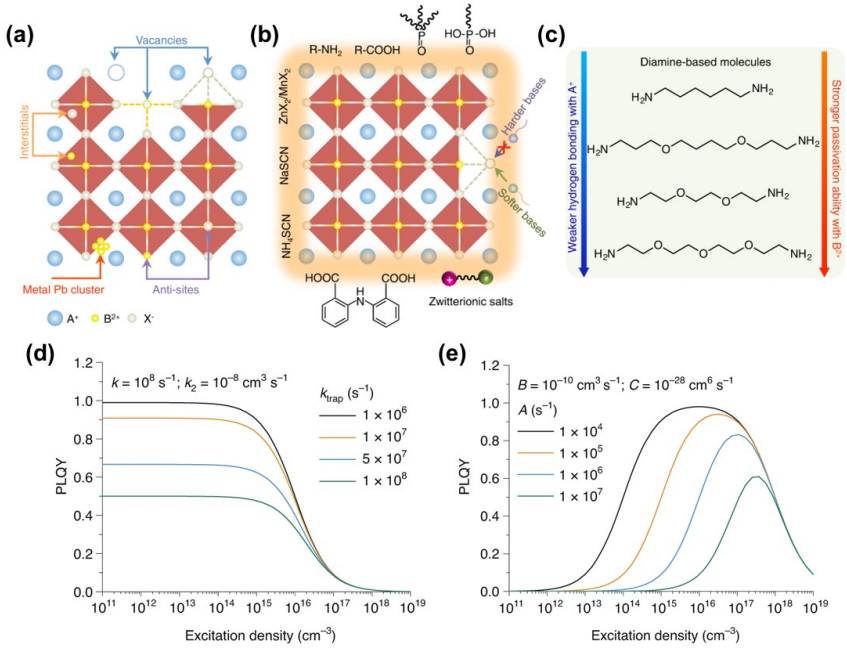

Figure 2. (**a**) Point defects in perovskites; (**b**) categories of passivating ligands for colloidal PNCs; (**c**) diamine-based molecules for perovskite passivation; related PLQY-excitation density plots with (**d**) varying trap-assisted nonradiative recombination rate constants in quantum-confined perovskites and (**e**) varying nonradiative monomolecular recombination coefficients in bulk perovskites. Figures adapted with permission from Springer Nature Ltd.

3. Blue Emission of LEDs

Component engineering of Cl and Br in the $CsPbBr_xCl_{3-x}$ and quantum confinement engineering of $CsPbBr_3$ to achieve a suitable bandgap for blue emitting are both effective strategies [69–71]. However, a mix of halides always results in phase separation and lattice distortion, which presents a negative effect on LEDs. In addition, Cl vacancies in mixed halide perovskites easily create relatively deeper defect levels in the bandgap, which could capture the carriers and increase the nonradiative recombination [72]. Moreover, the defects, which act as hoping sites to induce the halide ion migration and result in the perovskite being more vulnerable under operational conditions, have also been reported [73]. Compared with Cl vacancies in $CsPbBr_xCl_{3-x}$, the $CsPbBr_3$ exhibits strong "defect-tolerant" nature, which could reduce the related nonradiative recombination [74]. Therefore, the fabrication of quantum-confined $CsPbBr_3$, such as quasi-2D layers, nanoplatelets (NPs), and quantum dots (QDs), has attracted much attention for blue-emission LEDs. For achieving quantum-confined perovskites, ligands-assisted growth is an effective strategy and could fine-tune the size and even shape, resulting in a suitable bandgap for LED applications [75,76]. For example, the use of a cheap and facile solution-processable method to tune the emission of $MAPbBr_3$ from ~2.31 to 2.83 eV was reported by changing the organic ligand and its solute concentrations [77]. Quasi-2D $CsPbBr_3$-based perovskites with the formula of $A_2(CsPbBr_3)_{n-1}PbBr_4$, where A is an organic ammonium ligand and n is the phase order, have presented a high potential for the blue LED application because of high quantum confinement resulting in enlarging the bandgap from 2.4 to ~3.07 eV (determined by the n value) [78]. Using ligand engineering for the perovskite, the n phase could be controlled for blue emission. For example, mixed ligands of phenylethylammonium (PEA^+) and propylamine ion (PA^+) in perovskite solution could form $PEA_xPA_{2-x}(CsPbBr_3)_{n-1}PbBr_4$, which could inhibit the n = 2 phase generation and increase the n = 3 phase formation because of their thermodynamic stability differences (Figure 3a) [79,80]. The authors also introduced PEABr to passivate defects that are generated during perovskite crystallization. The PEABr-passivated $PEA_xPA_{2-x}(CsPbBr_3)_{n-1}PbBr_4$ exhibits an EQE of 7.51% and a brightness of 1765 cd m^{-2} and a low turn-on voltage of 3.07 V. Bifunctional ligands of 4-(2-aminoethyl)benzoic acid (ABA) [81] and γ-aminobutyric acid (GABA) [82] not only have a similar role for the quasi-2D phase engineering and passivating but also perform longer operational stability because of the strong interaction between perovskite phase [71]. $CsPbBr_3$ NPs with great quantum confinement effect have been synthesized with uniformly and precisely controllable thickness [83–85]. The thickness of $CsPbBr_3$ could be precisely controlled at a monolayer level for the blue LED design and fabrication [86]. However, the nucleation process of $CsPbBr_3$ could induce a large number of surface defects, such as Br vacancies, resulting in low EQE performance of the devices. To remove the surface defects of $CsPbBr_3$, HBr was employed in the perovskite precursor solution to increase Br- and eliminate Br vacancy [84]. Similarly, ligands, such as DDAB, 2,2-(ethylenedioxy) bis(ethylammonium) sulfate ($EDBESO_4$), and MABr [67,87,88], have been also utilized for the surface passivation in the $CsPbBr_3$ NPs-based LEDs for improving their performance. Moreover, ligands for the interfacial engineering and crystal growth controlling were also demonstrated (Figure 3b) [72,89,90], yet the EQE of the pure blue emission has not exceeded 2%. Compared with NPs, QDs-based $CsPbBr_3$ presents great progress and higher performance in the blue-emitting LEDs. C. Bi et al. employed $CsPbBr_3$ quantum dots with 4 nm size for blue PeLEDs fabrication, which exhibit great performance with an EQE of 4.7% with pure-blue emission at 470 nm, a brightness of 3850 cd m^{-2}, and a half-lifetime of 12 h, respectively. The results are attributed to the HBr etching imperfect octahedrons with vacancy defects and removing excess carboxylate ligands from the QDs surface. Auger recombination in the low-dimensional semiconductor easily occurs because of strongly bound excitons. A larger dielectric constant of inorganic ligands, such as $ZnBr_2$ and $ZnCl_2$, was induced in the quantum dot system to reduce the dielectric confinement and suppress Auger recombination [91,92]. $ZnBr_2$ with Br^- could also passivate uncoordinated sites and exchange with the initial organic ligands on the QDs surface to improve

the charge mobility between adjacent modified QDs [Figure 3c]. The resulted $CsPbBr_3$ QDs-based LED shows a pure-blue emission at 469 nm, low roll-off EQE, high luminance of 12,060 cd m^{-2}, and a high EQE of 10.3% (Figure 3d,e) [91]. Other effective strategies, including in-phase transformation from cubic to rhombic dodecahedron $CsPbBr_3$ QDs, on-substrate fabrication of QDs, and bipolar-shell resurfacing of QDs by ligands for blue LEDs application, have also exhibited great performance [28,48,93], strongly suggesting that $CsPbBr_3$ QDs provides more unique nature for the blue LED developments. Most of the important reports on the use of $CsPbBr_3$ NPL, quasi-2D, and QDs-emitting layers for blue LEDs have been summarized in Table 1.

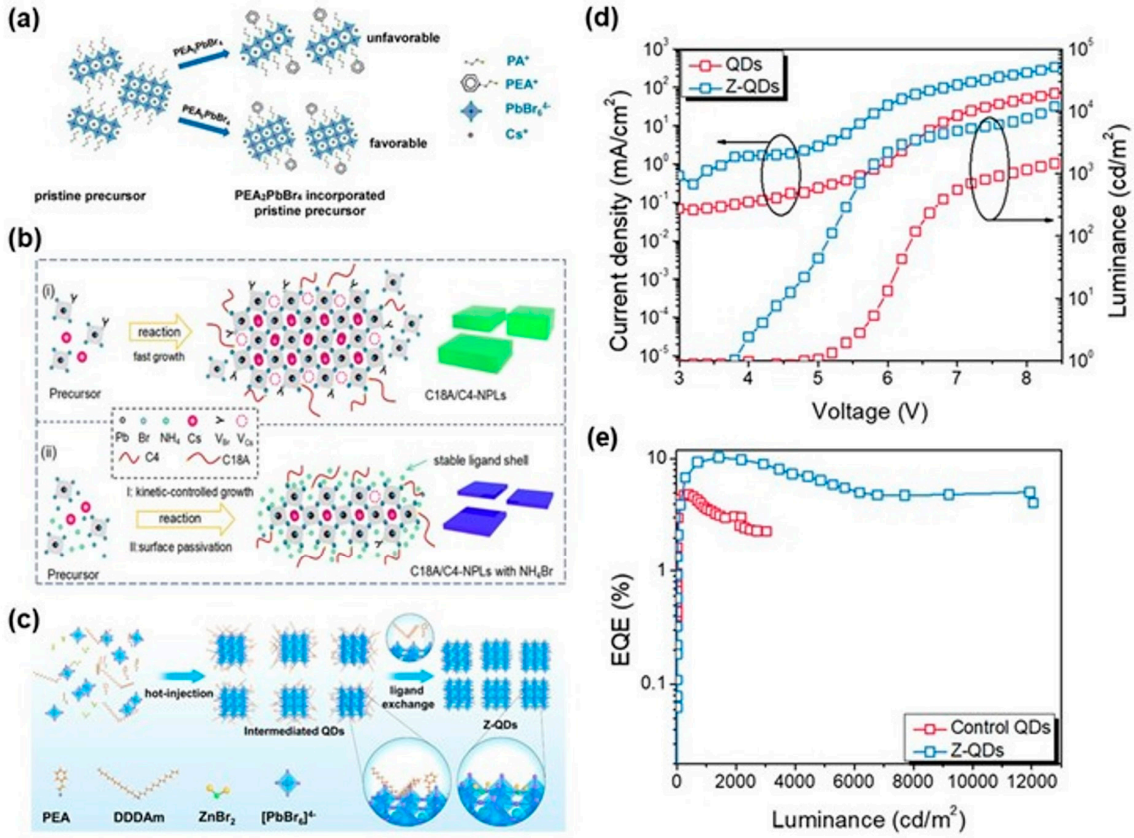

Figure 3. Schematic diagram of the effect of PEA_2PbBr_4 on the quasi-2D perovskite phases (**a**), C18A/C4 and NH^{4+}/C18A/C4 for $CsPbBr_3$ nanoplatelets (**b**), and $ZnBr_2$ for $CsPbBr_3$ QD modification (**c**). Current density, luminance (**d**), and EQE (**e**) of the $CsPbBr_3$ LEDs using $ZnBr_2$-modified QDs. Copyright from American Chemical Society.

Table 1. Summary of main blue LEDs based on the $CsPbBr_3$ NPL, quasi-2D, and QDs emitting layer.

Year	Emitting Layer	EQE (%)	Brightness (cd m^{-2})	EL Peak (nm)	Stability (min)	Ref.
2018	HBr-treated $CsPbBr_3$ NPL	0.124	62	463	-	[94]
2019	poly(triarylamine) modified $CsPbBr_3$ NPL	0.3	-	464	-	[89]
2019	DDAB-treated $CsPbBr_3$ NPL	1.42	41.8	469	0.7	[67]
2021	PEI-modified $CsPbBr_3$ NPL	0.8	631	465	-	[72]
2022	SA-modified $CsPbBr_3$ NPL	3.18	81.8	460	6.2	[88]
2022	NH_4Br- and PEABr-modified $CsPbBr_3$ NPL	2	74	463	-	[90]
2022	$EDBeSO_4$-modified $CsPbBr_3$ NPL	1.77	691	462	20	[87]
2019	$PA_2(CsPb\ Br_3)_{n-1}PbBr_4$	1.45	5735	487	220 at 150 cd m^{-2}	[80]

Table 1. *Cont.*

Year	Emitting Layer	EQE (%)	Brightness (cd m^{-2})	EL Peak (nm)	Stability (min)	Ref.
2020	$PEA_xPA_{2-x}(CsPbBr_3)_{n-1}PbBr_4$	7.51	1765	488	66	[79]
2020	GABA-treated $PEA_2(CsPbBr_3)_{n-1}PbBr_4$	6.3	200	478	2.5 at 200 cd m^{-2}	[82]
2020	ABA_2PbBr_4-modified $PEA_xPA_{2-x}(CsPbBr_3)_{n-1}PbBr_4$	11.1	513	486	81.3	[81]
2020	Bipolar-shell-protected 4 nm $CsPbBr_3$ QDs	12.3	~450	479	20 at 90 cd m^{-2}	[48]
2021	DDDAM- and PEA-treated 4 nm $CsPbBr_3$ QDs	4.7	3850	470	720	[73]
2022	$ZnBr_2$-treated 4 nm $CsPbBr_3$ QDs	10.3	12060	469	1500 at 115 cd m^{-2}	[91]
2022	Hydrobromide-treated $CsPbBr_3$ QDs	6.6	280.8	480	1.83 at 80 cd m^{-2}	[28]
2022	Br-MBA^+-treated $CsPbBr_3$ quantum dots	17.9%	~2500	480	120 at 100 cd m^{-2}	[93]

4. Stabilities of Materials and Devices

Compared with the other organic–inorganic halide perovskites, $CsPbBr_3$ presents good moisture, light, and thermal stability under a wide temperature range. $CsPbBr_3$ exhibiting better light stabilities than organic cation-based perovskites has been reported, and a comparison of the photostability of several typical halide perovskites is presented [95,96], implying that $CsPbBr_3$ could be better for the stabilized-light-involved devices. Akbulatov et al. performed comprehensive research on the photostability of different halide perovskites. The $CsPbBr_3$ film presents a higher degree of photostability without any prominent degradation, while the $MAPbBr_3$ exhibits serious degeneration under continuous illumination for 900 h [97]. Moreover, the $CsPbBr_3$ absorption bands increased even with long-term illumination, which also indicates the great photostability of the perovskite films. A comparison of the photostability of $MAPbI_3$, $MAPbBr_3$, and $CsPbBr_3$ was also conducted, which demonstrates that $CsPbBr_3$ displays superior stability compared with its counterparts. The photostability in the $CsPbBr_3$ QDs was also addressed [98], which indicates that the ligands-modified samples present much-improved photostability because of the elimination of the surface dangling bonds. Note that ligands on the QD surface could be eliminated because of the weak bound energy to QDs and dissolvability in a solvent, which could have a great impact on its stability. This phenomenon implies that the ligands are of great importance for the low dimensional perovskites [31]. In addition, the thermal and humidity stability of $CsPbBr_3$ have also been experimentally addressed, which shows negligible degradation below 350 °C and no evident change under the humidity of ~30% and temperature of ~25 °C [36,99]. The above-mentioned findings imply that Cs in the $CsPbBr_3$ could result in more suitable Goldschmidt tolerance and low formation energy of perovskite systems. Despite good stability of $CsPbBr_3$, its applications in the LEDs still show poor operational lifetime (T_{50} < 10 min, T_{50} is the time required for luminance to reach half of the initial value) [82,100]. The improved strategies, such as bipolar-shell QD fabrication, quasi-2D perovskites film formation, and interfacial engineering, have been reported [48,80,81]; however, the results are still far from our expectations (thousands of hours, or even over ten thousand hours). Very recently, the T_{50} lifetime presented a record value of over 30,000 h for green PLEDs at an initial luminance of 100 cd m^{-2}, which employed benzylphosphonic acid (BPA) additive for modifying three-dimensional polycrystalline perovskite films [101]. Another impressive report on the long operational stability is utilizing in situ solution-grown perovskite single crystals (SCs) for the LEDs, which enables great device performance with a high luminance of 86,000 cd m^{-2}, a peak external quantum efficiency of 11.2%, and a stability value of 12,500 h at an initial luminance of 100 cd m^{-2}, respectively [102]. These results imply that the bulk film with the passivated surface could greatly improve the stability of devices.

5. Perspectives and Summary

We have concluded that the ligand engineering for the achievement of great optical properties of $CsPbBr_3$ improved performances of $CsPbBr_3$-based blue LEDs and their stability. From the surface passivation and interfacial modification to the stabilization and quantum confinement of the perovskites, the ligands have demonstrated the great importance in the LED applications. Great achievements have been attained in $CsPbBr_3$-based LEDs, especially, their high EQE of green-emitting devices. Still, many crucial issues—such as the low efficiency of pure blue LEDs (center of emitting wavelength about 465 nm) and devices' operation stabilities—exist and need to be further addressed. The selected suitable ligands, which could eliminate the trap states in the perovskites with negligible effect on the carrier injection and radiative recombination, could further improve the EQE of the LEDs. The use of short organic or inorganic ligands, such as trimethylammonium, BPA, and $ZnBr_2$, could meet the requirements. For the stability of devices, most promising strategies should be the use of polycrystal bulk film or even single-crystal film with ligands-passivated surface for the device's fabrication [101,102], which could not only produce high performance but also reduce the efficiency roll-off because PLQY of single-crystal perovskites could realize nearly 100% at a wide range of excitation density (related to a broad range of bias voltage in LEDs) [62]. A universal strategy has been reported on preparing ultrathin $CsPbBr_3$ and other perovskites (Figure 4) [103], in which $CsPbBr_3$ with a thickness of 9.5 nm is greatly suitable for LED applications. With the technology and development of the perovskites, ligands, and combining the ligands with high-quality perovskites, high performance of perovskite-based LEDs with great EQE, brightness, and stability could be realized in the near future.

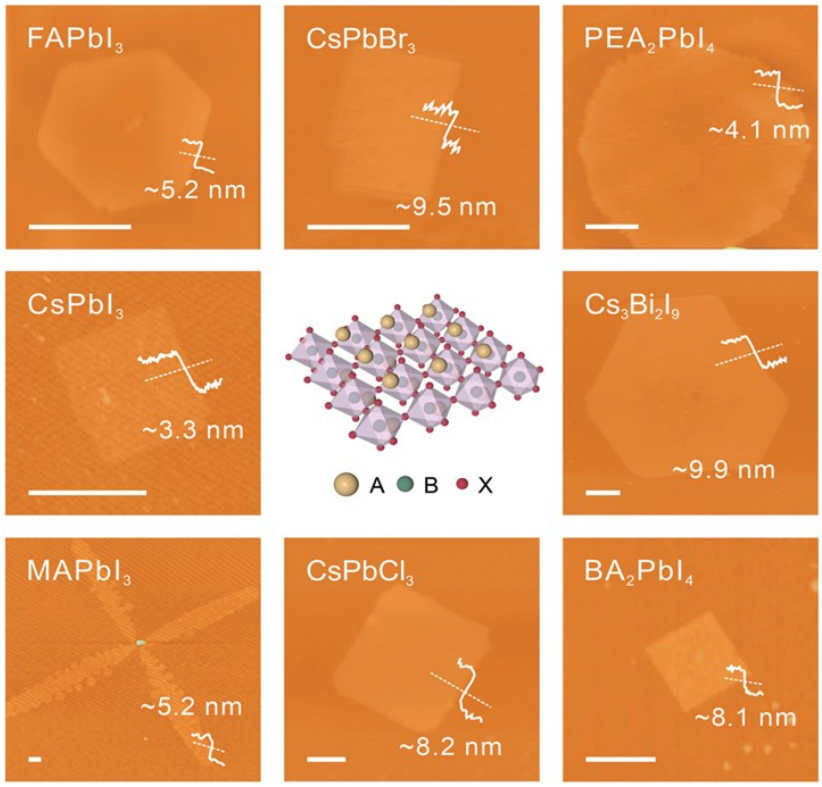

Figure 4. AFM topography images of the fabricated ultrathin perovskites by a universal strategy. Scale bar: 2 μm (A = organic/inorganic cation, B = metal cation and X = halide ion). Copyright from Wiley-VCH.

Funding: The authors gratefully acknowledge financial support from the National Natural Science Foundation of China (No.12174086).

Conflicts of Interest: The authors declare no conflict of interest.

References

1. Akkerman, Q.A.; Rainò, G.; Kovalenko, M.V.; Manna, L. Genesis, Challenges and Opportunities for Colloidal Lead Halide Perovskite Nanocrystals. *Nat. Mater.* **2018**, *17*, 394–405. [CrossRef] [PubMed]
2. Protesescu, L.; Yakunin, S.; Bodnarchuk, M.I.; Krieg, F.; Caputo, R.; Hendon, C.H.; Yang, R.X.; Walsh, A.; Kovalenko, M.V. Nanocrystals of Cesium Lead Halide Perovskites ($CsPbX_3$, X = Cl, Br, and I): Novel Optoelectronic Materials Showing Bright Emission with Wide Color Gamut. *Nano Lett.* **2015**, *15*, 3692–3696. [CrossRef] [PubMed]
3. Sun, C.; Zhang, Y.; Ruan, C.; Yin, C.; Wang, X.; Wang, Y.; Yu, W.W. Efficient and Stable White LEDs with Silica-Coated Inorganic Perovskite Quantum Dots. *Adv. Mater.* **2016**, *28*, 10088–10094. [CrossRef] [PubMed]
4. Liu, K.; Jiang, Y.; Jiang, Y.; Guo, Y.; Liu, Y.; Nakamura, E. Chemical Formation and Multiple Applications of Organic–Inorganic Hybrid Perovskite Materials. *J. Am. Chem. Soc.* **2019**, *141*, 1406–1414. [CrossRef] [PubMed]
5. Dai, S.; Hsu, B.; Chen, C.; Lee, C.; Liu, H.; Wang, H.; Huang, Y.; Wu, T.; Manikandan, A.; Ho, R.; et al. Perovskite Quantum Dots with Near Unity Solution and Neat-Film Photoluminescent Quantum Yield by Novel Spray Synthesis. *Adv. Mater.* **2018**, *30*, 1705532. [CrossRef]
6. Minh, D.N.; Kim, J.; Hyon, J.; Sim, J.H.; Sowlih, H.H.; Seo, C.; Nam, J.; Eom, S.; Suk, S.; Lee, S.; et al. Room-Temperature Synthesis of Widely Tunable Formamidinium Lead Halide Perovskite Nanocrystals. *Chem. Mater.* **2017**, *29*, 5713–5719. [CrossRef]
7. Chen, Q.; De Marco, N.; Yang, Y.; Song, T.-B.; Chen, C.-C.; Zhao, H.; Hong, Z.; Zhou, H.; Yang, Y. Under the Spotlight: The Organic–Inorganic Hybrid Halide Perovskite for Optoelectronic Applications. *Nano Today* **2015**, *10*, 355–396. [CrossRef]
8. Ding, J.; Yan, Q. Progress in Organic-Inorganic Hybrid Halide Perovskite Single Crystal: Growth Techniques and Applications. *Sci. China Mater.* **2017**, *60*, 1063–1078. [CrossRef]
9. Li, C.; Yang, J.; Su, F.; Tan, J.; Luo, Y.; Ye, S. Conformational Disorder of Organic Cations Tunes the Charge Carrier Mobility in Two-Dimensional Organic-Inorganic Perovskites. *Nat. Commun.* **2020**, *11*, 5481–5489. [CrossRef]
10. Juarez-Perez, E.J.; Hawash, Z.; Raga, S.R.; Ono, L.K.; Qi, Y. Thermal Degradation of $CH_3NH_3PbI_3$ Perovskite into NH_3 and CH_3I Gases Observed by Coupled Thermogravimetry–Mass Spectrometry Analysis. *Energy Environ. Sci.* **2016**, *9*, 3406–3410. [CrossRef]
11. Xiao, Z.; Song, Z.; Yan, Y. From Lead Halide Perovskites to Lead-Free Metal Halide Perovskites and Perovskite Derivatives. *Adv. Mater.* **2019**, *31*, 1803792. [CrossRef] [PubMed]
12. Shan, D.; Tong, G.; Cao, Y.; Tang, M.; Xu, J.; Yu, L.; Chen, K. The Effect of Decomposed PbI_2 on Microscopic Mechanisms of Scattering in $CH_3NH_3PbI_3$ Films. *Nanoscale Res. Lett.* **2019**, *14*, 208–214. [CrossRef] [PubMed]
13. Zhang, Z.; Fang, Z.; Guo, T.; Zhao, R.; Deng, Z.; Zhang, J.; Shang, M.; Liu, X.; Liu, J.; Huang, L.; et al. Robust Heterojunction to Strengthen the Performances of $FAPbI_3$ Perovskite Solar Cells. *Chem. Eng. J.* **2022**, *432*, 134311. [CrossRef]
14. Yan, F.; Tan, S.T.; Li, X.; Demir, H.V. Light Generation in Lead Halide Perovskite Nanocrystals: LEDs, Color Converters, Lasers, and Other Applications. *Small* **2019**, *15*, 1902079. [CrossRef] [PubMed]
15. Lu, M.; Guo, J.; Sun, S.; Lu, P.; Wu, J.; Wang, Y.; Kershaw, S.V.; Yu, W.W.; Rogach, A.L.; Zhang, Y. Bright $CsPbI_3$ Perovskite Quantum Dot Light-Emitting Diodes with Top-Emitting Structure and a Low Efficiency Roll-Off Realized by Applying Zirconium Acetylacetonate Surface Modification. *Nano Lett.* **2020**, *20*, 2829–2836. [CrossRef]
16. Zhang, C.; Wang, S.; Li, X.; Yuan, M.; Turyanska, L.; Yang, X. Core/Shell Perovskite Nanocrystals: Synthesis of Highly Efficient and Environmentally Stable $FAPbBr_3/CsPbBr_3$ for LED Applications. *Adv. Funct. Mater.* **2020**, *30*, 1910582. [CrossRef]
17. Wei, Y.; Cheng, Z.; Lin, J. An Overview on Enhancing the Stability of Lead Halide Perovskite Quantum Dots and Their Applications in Phosphor-Converted LEDs. *Chem. Soc. Rev.* **2019**, *48*, 310–350. [CrossRef]
18. Xie, K.; Wei, S.; Alhadhrami, A.; Liu, J.; Zhang, P.; Elnaggar, A.Y.; Zhang, F.; Mahmoud, M.H.H.; Murugadoss, V.; El-Bahy, S.M.; et al. Synthesis of $CsPbBr_3/CsPb_2Br_5$@Silica Yolk-Shell Composite Microspheres: Precisely Controllable Structure and Improved Catalytic Activity for Dye Degradation. *Adv. Compos. Hybrid Mater.* **2022**, *5*, 1423–1432. [CrossRef]
19. Liu, J.; Wu, Z.; Zhang, F.; Zhao, M.; Li, C.; Li, J.; Wen, B.; Wang, F. In Situ Growth of Lead-Free Halide Perovskites into SiO_2 Sub-Microcapsules Toward Water-Stable Photocatalytic CO_2 Reduction. *Nanoscale* **2023**, *15*, 7023–7031. [CrossRef]
20. Zhang, X.; Liu, H.; Wang, W.; Zhang, J.; Xu, B.; Karen, K.L.; Zheng, Y.; Liu, S.; Chen, S.; Wang, K.; et al. Hybrid Perovskite Light-Emitting Diodes Based on Perovskite Nanocrystals with Organic-Inorganic Mixed Cations. *Adv. Mater.* **2017**, *29*, 1606405. [CrossRef]
21. Amgar, D.; Binyamin, T.; Uvarov, V.; Etgar, L. Near Ultra-Violet to Mid-Visible Band Gap Tuning of Mixed Cation $Rb_xCs_{1-x}PbX_3$ (X = Cl or Br) Perovskite Nanoparticles. *Nanoscale* **2018**, *10*, 6060–6068. [CrossRef] [PubMed]
22. Huang, S.; Wang, B.; Zhang, Q.; Li, Z.; Shan, A.; Li, L. Postsynthesis Potassium-Modification Method to Improve Stability of $CsPbBr_3$ Perovskite Nanocrystals. *Adv. Opt. Mater.* **2018**, *6*, 1701106. [CrossRef]
23. Tong, G.; Ono, L.K.; Qi, Y. Recent Progress of All-Bromide Inorganic Perovskite Solar Cells. *Energy Technol.-Ger.* **2020**, *8*, 1900961. [CrossRef]

24. Nenon, D.P.; Pressler, K.; Kang, J.; Koscher, B.A.; Olshansky, J.H.; Osowiecki, W.T.; Koc, M.A.; Wang, L.-W.; Alivisatos, A.P. Design Principles for Trap-Free $CsPbX_3$ Nanocrystals: Enumerating and Eliminating Surface Halide Vacancies with Softer Lewis Bases. *J. Am. Chem. Soc.* **2018**, *140*, 17760–17772. [CrossRef] [PubMed]
25. Shi, S.; Wang, Y.; Zeng, S.; Cui, Y.; Xiao, Y. Surface Regulation of $CsPbBr_3$ Quantum Dots for Standard Blue-Emission with Boosted PLQY. *Adv. Opt. Mater.* **2020**, *8*, 2000167. [CrossRef]
26. Li, X.; Wu, Y.; Zhang, S.; Cai, B.; Gu, Y.; Song, J.; Zeng, H. $CsPbX_3$ Quantum Dots for Lighting and Displays: Room-Temperature Synthesis, Photoluminescence Superiorities, Underlying Origins and White Light-Emitting Diodes. *Adv. Funct. Mater.* **2016**, *26*, 2435–2445. [CrossRef]
27. Shamsi, J.; Kubicki, D.; Anaya, M.; Liu, Y.; Ji, K.; Frohna, K.; Grey, C.P.; Friend, R.H.; Stranks, S.D. Stable Hexylphosphonate-Capped Blue-Emitting Quantum-Confined $CsPbBr_3$ Nanoplatelets. *ACS Energy Lett.* **2020**, *5*, 1900–1907. [CrossRef]
28. Yuan, L.; Li, D.; Liu, H.; Zhang, F.; Wang, S. Quantum-Confined Dodecahedron $CsPbBr_3$ Quantum Dots by A Sequential Post-Treatment Strategy for Efficient Blue PeLEDs. *Adv. Funct. Mater.* **2022**, *32*, 2208065. [CrossRef]
29. Li, Y.; Huang, H.; Xiong, Y.; Kershaw, S.V.; Rogach, A.L. Reversible Transformation Between $CsPbBr_3$ and Cs_4PbBr_6 Nanocrystals. *CrystEngComm* **2018**, *20*, 4900–4904. [CrossRef]
30. Zhang, D.; Yang, Y.; Bekenstein, Y.; Yu, Y.; Gibson, N.A.; Wong, A.B.; Eaton, S.W.; Kornienko, N.; Kong, Q.; Lai, M.; et al. Synthesis of Composition Tunable and Highly Luminescent Cesium Lead Halide Nanowires through Anion-Exchange Reactions. *J. Am. Chem. Soc.* **2016**, *138*, 7236–7241. [CrossRef]
31. Ullah, S.; Wang, J.; Yang, P.; Liu, L.; Yang, S.-E.; Xia, T.; Guo, H.; Chen, Y. All-inorganic $CsPbBr_3$ Perovskite: A Promising Choice for Photovoltaics. *Mater. Adv.* **2021**, *2*, 646–683. [CrossRef]
32. Swarnkar, A.; Mir, W.J.; Nag, A. Can B-Site Doping or Alloying Improve Thermal- and Phase-Stability of All-Inorganic $CsPbX_3$ (X = Cl, Br, I) Perovskites? *ACS Energy Lett.* **2018**, *3*, 286–289. [CrossRef]
33. Hirotsu, S.; Harada, J.; Iizumi, M.; Gesi, K. Structural Phase Transitions in $CsPbBr_3$. *J. Phys. Soc. Jpn.* **1974**, *37*, 1393–1398. [CrossRef]
34. Akbali, B.; Topcu, G.; Guner, T.; Ozcan, M.; Demir, M.M.; Sahin, H. $CsPbBr_3$ perovskites: Theoretical and Experimental Investigation on Water-Assisted Transition from Nanowire Formation to Degradation. *Phys. Rev. Mater.* **2018**, *2*, 034601. [CrossRef]
35. Stoumpos, C.C.; Malliakas, C.D.; Peters, J.A.; Liu, Z.; Sebastian, M.; Im, J.; Chasapis, T.C.; Wibowo, A.C.; Chung, D.Y.; Freeman, A.J.; et al. Crystal Growth of the Perovskite Semiconductor $CsPbBr_3$: A New Material for High-Energy Radiation Detection. *Cryst. Growth Des.* **2013**, *13*, 2722–2727. [CrossRef]
36. Sutton, R.J.; Eperon, G.E.; Miranda, L.; Parrott, E.S.; Kamino, B.A.; Patel, J.B.; Hörantner, M.T.; Johnston, M.B.; Haghighirad, A.A.; Moore, D.T.; et al. Bandgap-Tunable Cesium Lead Halide Perovskites with High Thermal Stability for Efficient Solar Cells. *Adv. Energy Mater.* **2016**, *6*, 1502458. [CrossRef]
37. Ghaithan, H.M.; Alahmed, Z.A.; Qaid, S.M.H.; Hezam, M.; Aldwayyan, A.S. Density Functional Study of Cubic, Tetragonal, and Orthorhombic $CsPbBr_3$ Perovskite. *ACS Omega* **2020**, *5*, 7468–7480. [CrossRef]
38. Maes, J.; Balcaen, L.; Drijvers, E.; Zhao, Q.; De Roo, J.; Vantomme, A.; Vanhaecke, F.; Geiregat, P.; Hens, Z. Light Absorption Coefficient of $CsPbBr_3$ Perovskite Nanocrystals. *J. Phys. Chem. Lett.* **2018**, *9*, 3093–3097. [CrossRef]
39. Yettapu, G.R.; Talukdar, D.; Sarkar, S.; Swarnkar, A.; Nag, A.; Ghosh, P.; Mandal, P. Terahertz Conductivity within Colloidal $CsPbBr_3$ Perovskite Nanocrystals: Remarkably High Carrier Mobilities and Large Diffusion Lengths. *Nano Lett.* **2016**, *16*, 4838–4848. [CrossRef]
40. Kang, Y.; Han, S. Intrinsic Carrier Mobility of Cesium Lead Halide Perovskites. *Phys. Rev. Appl.* **2018**, *10*, 044013. [CrossRef]
41. Song, J.; Cui, Q.; Li, J.; Xu, J.; Wang, Y.; Xu, L.; Xue, J.; Dong, Y.; Tian, T.; Sun, H.; et al. Ultralarge All-Inorganic Perovskite Bulk Single Crystal for High-Performance Visible–Infrared Dual-Modal Photodetectors. *Adv. Opt. Mater.* **2017**, *5*, 1700157. [CrossRef]
42. Lin, K.; Xing, J.; Quan, L.N.; de Arquer, F.P.G.; Gong, X.; Lu, J.; Xie, L.; Zhao, W.; Zhang, D.; Yan, C.; et al. Perovskite Light-Emitting Diodes with External Quantum Efficiency Exceeding 20 Per Cent. *Nature* **2018**, *562*, 245–248. [CrossRef] [PubMed]
43. Wan, Q.; Zheng, W.; Zou, C.; Carulli, F.; Zhang, C.; Song, H.; Liu, M.; Zhang, Q.; Lin, L.Y.; Kong, L.; et al. Ultrathin Light-Emitting Diodes with External Efficiency over 26% Based on Resurfaced Perovskite Nanocrystals. *ACS Energy Lett.* **2023**, *8*, 927–934. [CrossRef]
44. Zhang, X.; Shi, L.; Bai, J.; Wang, F.; Jiang, M. Heterointerface Engineering of Perovskite Defects and Energetics for Light-Emitting Diodes. *Nano Res.* **2023**, *16*, 5525–5532. [CrossRef]
45. Kong, L.; Luo, Y.; Turyanska, L.; Zhang, T.; Zhang, Z.; Xing, G.; Yang, Y.; Zhang, C.; Yang, X. A Spacer Cation Assisted Nucleation and Growth Strategy Enables Efficient and High-Luminance Quasi-2D Perovskite LEDs. *Adv. Funct. Mater.* **2022**, *33*, 2209186. [CrossRef]
46. Jiang, M.; Zhang, X.; Wang, F. Enabling Monodisperse Perovskite Phase with Buried Interface Modification Toward Efficient Light-Emitting Diodes. *Nano Res. Energy* **2023**, *2*, e9120069. [CrossRef]
47. Pan, J.; Quan, L.N.; Zhao, Y.; Peng, W.; Murali, B.; Sarmah, S.P.; Yuan, M.; Sinatra, L.; Alyami, N.M.; Liu, J.; et al. Highly Efficient Perovskite-Quantum-Dot Light-Emitting Diodes by Surface Engineering. *Adv. Mater.* **2016**, *28*, 8718–8725. [CrossRef] [PubMed]
48. Dong, Y.; Wang, Y.K.; Yuan, F.; Johnston, A.; Liu, Y.; Ma, D.; Choi, M.J.; Chen, B.; Chekini, M.; Baek, S.W.; et al. Bipolar-Shell Resurfacing for Blue LEDs Based on Strongly Confined Perovskite Quantum Dots. *Nat. Nanotechnol.* **2020**, *15*, 668–674. [CrossRef]

49. Koscher, B.A.; Swabeck, J.K.; Bronstein, N.D.; Alivisatos, A.P. Essentially Trap-Free $CsPbBr_3$ Colloidal Nanocrystals by Postsynthetic Thiocyanate Surface Treatment. *J. Am. Chem. Soc.* **2017**, *139*, 6566–6569. [CrossRef]
50. Song, J.; Li, J.; Li, X.; Xu, L.; Dong, Y.; Zeng, H. Quantum Dot Light-Emitting Diodes Based on Inorganic Perovskite Cesium Lead Halides ($CsPbX_3$). *Adv. Mater.* **2015**, *27*, 7162–7167. [CrossRef]
51. Wang, Z.; Wang, F.; Sun, W.; Ni, R.; Hu, S.; Liu, J.; Zhang, B.; Alsaed, A.; Hayat, T.; Tan, Z.a. Manipulating the Trade-off Between Quantum Yield and Electrical Conductivity for High-Brightness Quasi-2D Perovskite Light-Emitting Diodes. *Adv. Funct. Mater.* **2018**, *28*, 1804187. [CrossRef]
52. Li, J.; Xu, L.; Wang, T.; Song, J.; Chen, J.; Xue, J.; Dong, Y.; Cai, B.; Shan, Q.; Han, B.; et al. 50-Fold EQE Improvement up to 6.27% of Solution-Processed All-Inorganic Perovskite $CsPbBr_3$ QLEDs via Surface Ligand Density Control. *Adv. Mater.* **2017**, *29*, 1603885. [CrossRef] [PubMed]
53. Song, J.; Li, J.; Xu, L.; Li, J.; Zhang, F.; Han, B.; Shan, Q.; Zeng, H. Room-Temperature Triple-Ligand Surface Engineering Synergistically Boosts Ink Stability, Recombination Dynamics, and Charge Injection toward EQE-11.6% Perovskite QLEDs. *Adv. Mater.* **2018**, *30*, 1800764. [CrossRef] [PubMed]
54. Chiba, T.; Hoshi, K.; Pu, Y.J.; Takeda, Y.; Hayashi, Y.; Ohisa, S.; Kawata, S.; Kido, J. High-Efficiency Perovskite Quantum-Dot Light-Emitting Devices by Effective Washing Process and Interfacial Energy Level Alignment. *ACS Appl. Mater. Interfaces* **2017**, *9*, 18054–18060. [CrossRef]
55. Chen, H.; Fan, L.; Zhang, R.; Liu, W.; Zhang, Q.; Guo, R.; Zhuang, S.; Wang, L. Sodium Ion Modifying In Situ Fabricated $CsPbBr_3$ Nanoparticles for Efficient Perovskite Light Emitting Diodes. *Adv. Opt. Mater.* **2019**, *7*, 1900747. [CrossRef]
56. Wang, H.; Zhang, X.; Wu, Q.; Cao, F.; Yang, D.; Shang, Y.; Ning, Z.; Zhang, W.; Zheng, W.; Yan, Y.; et al. Trifluoroacetate Induced Small-Grained $CsPbBr_3$ Perovskite Films Result in Efficient and Stable Light-Emitting Devices. *Nat. Commun.* **2019**, *10*, 665–675. [CrossRef]
57. Cui, J.; Liu, Y.; Deng, Y.; Lin, C.; Fang, Z.; Xiang, C.; Bai, P.; Du, K.; Zuo, X.; Wen, K.; et al. Efficient Light-Emitting Diodes Based on Oriented Perovskite Nanoplatelets. *Sci. Adv.* **2021**, *7*, 8458–8465. [CrossRef]
58. Meggiolaro, D.; Motti, S.G.; Mosconi, E.; Barker, A.J.; Ball, J.; Andrea Riccardo Perini, C.; Deschler, F.; Petrozza, A.; De Angelis, F. Lodine Chemistry Determines the Defect Tolerance of Lead-Halide Perovskites. *Energy Environ. Sci.* **2018**, *11*, 702–713. [CrossRef]
59. Pandey, M.; Rasmussen, F.A.; Kuhar, K.; Olsen, T.; Jacobsen, K.W.; Thygesen, K.S. Defect-Tolerant Monolayer Transition Metal Dichalcogenides. *Nano Lett.* **2016**, *16*, 2234–2240. [CrossRef]
60. Chen, B.; Rudd, P.N.; Yang, S.; Yuan, Y.; Huang, J. Imperfections and Their Passivation in Halide Perovskite Solar Cells. *Chem. Soc. Rev.* **2019**, *48*, 3842–3867. [CrossRef]
61. Ball, J.M.; Petrozza, A. Defects in Perovskite-Halides and Their Effects in Solar Cells. *Nat. Energy* **2016**, *1*, 16149–16162. [CrossRef]
62. Liu, X.; Xu, W.; Bai, S.; Jin, Y.; Wang, J.; Friend, R.H.; Gao, F. Metal Halide Perovskites for Light-Emitting Diodes. *Nat. Mater.* **2021**, *20*, 10–21. [CrossRef] [PubMed]
63. de Quilettes, D.W.; Koch, S.; Burke, S.; Paranji, R.K.; Shropshire, A.J.; Ziffer, M.E.; Ginger, D.S. Photoluminescence Lifetimes Exceeding 8 µs and Quantum Yields Exceeding 30% in Hybrid Perovskite Thin Films by Ligand Passivation. *ACS Energy Lett.* **2016**, *1*, 438–444. [CrossRef]
64. Song, L.; Guo, X.; Hu, Y.; Lv, Y.; Lin, J.; Liu, Z.; Fan, Y.; Liu, X. Efficient Inorganic Perovskite Light-Emitting Diodes with Polyethylene Glycol Passivated Ultrathin $CsPbBr_3$ Films. *J. Phys. Chem. Lett.* **2017**, *8*, 4148–4154. [CrossRef]
65. Wu, C.; Zou, Y.; Wu, T.; Ban, M.; Pecunia, V.; Han, Y.; Liu, Q.; Song, T.; Duhm, S.; Sun, B. Improved Performance and Stability of All-Inorganic Perovskite Light-Emitting Diodes by Antisolvent Vapor Treatment. *Adv. Funct. Mater.* **2017**, *27*, 1700338. [CrossRef]
66. Krieg, F.; Ochsenbein, S.T.; Yakunin, S.; Ten Brinck, S.; Aellen, P.; Suess, A.; Clerc, B.; Guggisberg, D.; Nazarenko, O.; Shynkarenko, Y.; et al. Colloidal $CsPbX_3$ (X = Cl, Br, I) Nanocrystals 2.0: Zwitterionic Capping Ligands for Improved Durability and Stability. *ACS Energy Lett.* **2018**, *3*, 641–646. [CrossRef] [PubMed]
67. Zhang, C.; Wan, Q.; Wang, B.; Zheng, W.; Liu, M.; Zhang, Q.; Kong, L.; Li, L. Surface Ligand Engineering toward Brightly Luminescent and Stable Cesium Lead Halide Perovskite Nanoplatelets for Efficient Blue-Light-Emitting Diodes. *J. Phys. Chem. C.* **2019**, *123*, 26161–26169. [CrossRef]
68. Bae, W.K.; Park, Y.S.; Lim, J.; Lee, D.; Padilha, L.A.; McDaniel, H.; Robel, I.; Lee, C.; Pietryga, J.M.; Klimov, V.I. Controlling the Influence of Auger Recombination on the Performance of Quantum-Dot Light-Emitting Diodes. *Nat. Commun.* **2013**, *4*, 2661–2669. [CrossRef]
69. Liu, B.; Li, J.; Wang, G.; Ye, F.; Yan, H.; Zhang, M.; Dong, S.-C.; Lu, L.; Huang, P.; He, T.; et al. Lattice Strain Modulation Toward Efficient Blue Perovskite Light-Emitting Diodes. *Sci. Adv.* **2022**, *8*, 0138–0146. [CrossRef]
70. Li, Z.; Chen, Z.; Yang, Y.; Xue, Q.; Yip, H.L.; Cao, Y. Modulation of Recombination Zone Position for Quasi-Two-Dimensional Blue Perovskite Light-Emitting Diodes with Efficiency Exceeding 5%. *Nat. Commun.* **2019**, *10*, 1027–1037. [CrossRef]
71. Ahmad, S.; Fu, P.; Yu, S.; Yang, Q.; Liu, X.; Wang, X.; Wang, X.; Guo, X.; Li, C. Dion-Jacobson Phase 2D Layered Perovskites for Solar Cells with Ultrahigh Stability. *Joule* **2019**, *3*, 794–806. [CrossRef]
72. Yin, W.; Li, M.; Dong, W.; Luo, Z.; Li, Y.; Qian, J.; Zhang, J.; Zhang, W.; Zhang, Y.; Kershaw, S.V.; et al. Multidentate Ligand Polyethylenimine Enables Bright Color-Saturated Blue Light-Emitting Diodes Based on $CsPbBr_3$ Nanoplatelets. *ACS Energy Lett.* **2021**, *6*, 477–484. [CrossRef]

73. Bi, C.; Yao, Z.; Sun, X.; Wei, X.; Wang, J.; Tian, J. Perovskite Quantum Dots with Ultralow Trap Density by Acid Etching-Driven Ligand Exchange for High Luminance and Stable Pure-Blue Light-Emitting Diodes. *Adv. Mater.* **2021**, *33*, 2006722. [CrossRef] [PubMed]
74. Pan, J.; Li, X.; Gong, X.; Yin, J.; Zhou, D.; Sinatra, L.; Huang, R.; Liu, J.; Chen, J.; Dursun, I.; et al. Halogen Vacancies Enable Ligand-Assisted Self-Assembly of Perovskite Quantum Dots into Nanowires. *Angew. Chem. Int. Ed.* **2019**, *58*, 16077–16081. [CrossRef]
75. Adhikari, G.C.; Vargas, P.A.; Zhu, H.; Grigoriev, A.; Zhu, P. Tetradic Phosphor White Light with Variable CCT and Superlative CRI through Organolead Halide Perovskite Nanocrystals. *Nanoscale Adv.* **2019**, *1*, 1791–1798. [CrossRef]
76. Park, M.-H. 3D and 2D Metal Halide Perovskites for Blue Light-Emitting Diodes. *Materials* **2022**, *15*, 4571. [CrossRef]
77. Adhikari, G.C.; Zhu, H.; Vargas, P.A.; Zhu, P. UV-Green Emission from Organolead Bromide Perovskite Nanocrystals. *J. Phys. Chem. C* **2018**, *122*, 15041–15046. [CrossRef]
78. Chen, C.; Zeng, L.; Jiang, Z.; Xu, Z.; Chen, Y.; Wang, Z.; Chen, S.; Xu, B.; Mai, Y.; Guo, F. Vacuum-Assisted Preparation of High-Quality Quasi-2D Perovskite Thin Films for Large-Area Light-Emitting Diodes. *Adv. Funct. Mater.* **2022**, *32*, 2107644. [CrossRef]
79. Ren, Z.; Li, L.; Yu, J.; Ma, R.; Xiao, X.; Chen, R.; Wang, K.; Sun, X.W.; Yin, W.-J.; Choy, W.C.H. Simultaneous Low-Order Phase Suppression and Defect Passivation for Efficient and Stable Blue Light-Emitting Diodes. *ACS Energy Lett.* **2020**, *5*, 2569–2579. [CrossRef]
80. Ren, Z.; Xiao, X.; Ma, R.; Lin, H.; Wang, K.; Sun, X.W.; Choy, W.C.H. Hole Transport Bilayer Structure for Quasi-2D Perovskite Based Blue Light-Emitting Diodes with High Brightness and Good Spectral Stability. *Adv. Funct. Mater.* **2019**, *29*, 1905339. [CrossRef]
81. Ren, Z.; Yu, J.; Qin, Z.; Wang, J.; Sun, J.; Chan, C.C.S.; Ding, S.; Wang, K.; Chen, R.; Wong, K.S.; et al. High-Performance Blue Perovskite Light-Emitting Diodes Enabled by Efficient Energy Transfer between Coupled Quasi-2D Perovskite Layers. *Adv. Mater.* **2021**, *33*, 2005570. [CrossRef]
82. Wang, Y.K.; Ma, D.; Yuan, F.; Singh, K.; Pina, J.M.; Johnston, A.; Dong, Y.; Zhou, C.; Chen, B.; Sun, B.; et al. Chelating-Agent-Assisted Control of $CsPbBr_3$ Quantum Well Growth Enables Stable Blue Perovskite Emitters. *Nat. Commun.* **2020**, *11*, 3674–3681. [CrossRef]
83. Bekenstein, Y.; Koscher, B.A.; Eaton, S.W.; Yang, P.; Alivisatos, A.P. Highly Luminescent Colloidal Nanoplates of Perovskite Cesium Lead Halide and Their Oriented Assemblies. *J. Am. Chem. Soc.* **2015**, *137*, 16008–16011. [CrossRef]
84. Song, J.; Xu, L.; Li, J.; Xue, J.; Dong, Y.; Li, X.; Zeng, H. Monolayer and Few-Layer All-Inorganic Perovskites as a New Family of Two-Dimensional Semiconductors for Printable Optoelectronic Devices. *Adv. Mater.* **2016**, *28*, 4861–4869. [CrossRef] [PubMed]
85. Akkerman, Q.A.; Motti, S.G.; Srimath Kandada, A.R.; Mosconi, E.; D'Innocenzo, V.; Bertoni, G.; Marras, S.; Kamino, B.A.; Miranda, L.; De Angelis, F.; et al. Solution Synthesis Approach to Colloidal Cesium Lead Halide Perovskite Nanoplatelets with Monolayer-Level Thickness Control. *J. Am. Chem. Soc.* **2016**, *138*, 1010–1016. [CrossRef]
86. Yang, D.; Zou, Y.; Li, P.; Liu, Q.; Wu, L.; Hu, H.; Xu, Y.; Sun, B.; Zhang, Q.; Lee, S.-T. Large-Scale Synthesis of Ultrathin Cesium Lead Bromide Perovskite Nanoplates with Precisely Tunable Dimensions and Their Application in Blue Light-Emitting Diodes. *Nano Energy* **2018**, *47*, 235–242. [CrossRef]
87. Liu, H.; Worku, M.; Mondal, A.; Shonde, T.B.; Chaaban, M.; Ben-Akacha, A.; Lee, S.; Gonzalez, F.; Olasupo, O.; Lin, X.; et al. Efficient and Stable Blue Light Emitting Diodes Based on $CsPbBr_3$ Nanoplatelets with Surface Passivation by Multifunctional Organic Sulfate. *Adv. Energy Mater.* **2022**, *12*, 2201605. [CrossRef]
88. Shen, W.; Yu, Y.; Zhang, W.; Chen, Y.; Zhang, J.; Yang, L.; Feng, J.; Cheng, G.; Liu, L.; Chen, S. Efficient Pure Blue Light-Emitting Diodes Based on $CsPbBr_3$ Quantum-Confined Nanoplates. *ACS Appl. Mater. Interfaces* **2022**, *14*, 5682–5691. [CrossRef] [PubMed]
89. Hoye, R.L.Z.; Lai, M.L.; Anaya, M.; Tong, Y.; Galkowski, K.; Doherty, T.; Li, W.; Huq, T.N.; Mackowski, S.; Polavarapu, L.; et al. Identifying and Reducing Interfacial Losses to Enhance Color-Pure Electroluminescence in Blue-Emitting Perovskite Nanoplatelet Light-Emitting Diodes. *ACS Energy Lett.* **2019**, *4*, 1181–1188. [CrossRef]
90. Wang, H.; Ye, F.; Sun, J.; Wang, Z.; Zhang, C.; Qian, J.; Zhang, X.; Choy, W.C.H.; Sun, X.W.; Wang, K.; et al. Efficient $CsPbBr_3$ Nanoplatelet-Based Blue Light-Emitting Diodes Enabled by Engineered Surface Ligands. *ACS Energy Lett.* **2022**, *7*, 1137–1145. [CrossRef]
91. Bi, C.; Yao, Z.; Hu, J.; Wang, X.; Zhang, M.; Tian, S.; Liu, A.; Lu, Y.; de Leeuw, N.H.; Sui, M.; et al. Suppressing Auger Recombination of Perovskite Quantum Dots for Efficient Pure-Blue-Light-Emitting Diodes. *ACS Energy Lett.* **2022**, *8*, 731–739. [CrossRef]
92. Yao, Z.; Bi, C.; Liu, A.; Zhang, M.; Tian, J. High Brightness and Stability Pure-Blue Perovskite Light-Emitting Diodes Based on a Novel Structural Quantum-Dot Film. *Nano Energy* **2022**, *95*, 106982. [CrossRef]
93. Jiang, Y.; Sun, C.; Xu, J.; Li, S.; Cui, M.; Fu, X.; Liu, Y.; Liu, Y.; Wan, H.; Wei, K.; et al. Synthesis-on-Substrate of Quantum Dot Solids. *Nature* **2022**, *612*, 679–684. [CrossRef] [PubMed]
94. Wu, Y.; Wei, C.; Li, X.; Li, Y.; Qiu, S.; Shen, W.; Cai, B.; Sun, Z.; Yang, D.; Deng, Z.; et al. In Situ Passivation of $[PbBr_6]^{4-}$ Octahedra toward Blue Luminescent $CsPbBr_3$ Nanoplatelets with Near 100% Absolute Quantum Yield. *ACS Energy Lett.* **2018**, *3*, 2030–2037. [CrossRef]
95. Klein-Kedem, N.; Cahen, D.; Hodes, G. Effects of Light and Electron Beam Irradiation on Halide Perovskites and Their Solar Cells. *Acc. Chem. Res.* **2016**, *49*, 347–354. [CrossRef]

96. Zhou, W.; Zhao, Y.; Zhou, X.; Fu, R.; Li, Q.; Zhao, Y.; Liu, K.; Yu, D.; Zhao, Q. Light-Independent Ionic Transport in Inorganic Perovskite and Ultrastable Cs-Based Perovskite Solar Cells. *J. Phys. Chem. Lett.* **2017**, *8*, 4122–4128. [CrossRef]
97. Akbulatov, A.F.; Luchkin, S.Y.; Frolova, L.A.; Dremova, N.N.; Gerasimov, K.L.; Zhidkov, I.S.; Anokhin, D.V.; Kurmaev, E.Z.; Stevenson, K.J.; Troshin, P.A. Probing the Intrinsic Thermal and Photochemical Stability of Hybrid and Inorganic Lead Halide Perovskites. *J. Phys. Chem. Lett.* **2017**, *8*, 1211–1218. [CrossRef]
98. Chen, J.; Liu, D.; Al-Marri, M.J.; Nuuttila, L.; Lehtivuori, H.; Zheng, K. Photo-Stability of CsPbBr3 Perovskite Quantum Dots for Optoelectronic Application. *Sci. China Mater.* **2016**, *59*, 719–727. [CrossRef]
99. Cao, X.; Zhang, G.; Jiang, L.; Cai, Y.; Gao, Y.; Yang, W.; He, X.; Zeng, Q.; Xing, G.; Jia, Y.; et al. Water, a Green Solvent for Fabrication of High-Quality $CsPbBr_3$ Films for Efficient Solar Cells. *ACS Appl. Mater. Interfaces* **2020**, *12*, 5925–5931. [CrossRef]
100. Dyrvik, E.G.; Warby, J.H.; McCarthy, M.M.; Ramadan, A.J.; Zaininger, K.A.; Lauritzen, A.E.; Mahesh, S.; Taylor, R.A.; Snaith, H.J. Reducing Nonradiative Losses in Perovskite LEDs through Atomic Layer Deposition of Al_2O_3 on the Hole-Injection Contact. *ACS Nano* **2023**, *17*, 3289–3300. [CrossRef]
101. Kim, J.S.; Heo, J.M.; Park, G.S.; Woo, S.J.; Cho, C.; Yun, H.J.; Kim, D.H.; Park, J.; Lee, S.C.; Park, S.H.; et al. Ultra-Bright, Efficient and Stable Perovskite Light-Emitting Diodes. *Nature* **2022**, *611*, 688–694. [CrossRef] [PubMed]
102. Chen, W.; Huang, Z.; Yao, H.; Liu, Y.; Zhang, Y.; Li, Z.; Zhou, H.; Xiao, P.; Chen, T.; Sun, H.; et al. Highly Bright and Stable Single-Crystal Perovskite Light-Emitting Diodes. *Nat. Photonics* **2023**, *17*, 401–407. [CrossRef]
103. Li, L.; Yu, Y.; Li, P.; Liu, J.; Liang, L.; Wang, L.; Ding, Y.; Han, X.; Ji, J.; Chen, S.; et al. The Universal Growth of Ultrathin Perovskite Single Crystals. *Adv. Mater.* **2022**, *34*, 2108396. [CrossRef] [PubMed]